Peroxyacetyl nitrate measurements by thermal dissociation–chemical ionization mass spectrometry in an urban environment: Performance and characterizations

Running head: Peroxyacetyl nitrate measurements by TD-CIMS in an urban environment

Xinfeng WANG[1], Tao WANG[1,2], Likun XUE (✉)[1], Wei NIE[3], Zheng XU[3], Steven C.N. POON[2], Wenxing WANG[1]

1 Environment Research Institute, Shandong University, Ji'nan 250100, China

2 Department of Civil and Environmental Engineering, Hong Kong Polytechnic University, Hong Kong, China

3 Institute for Climate and Global Change Research & School of Atmospheric Sciences, Nanjing University, Nanjing, 210023, China

✉ Corresponding author

Email: xuelikun@sdu.edu.cn

Highlights

- The loss degree of PAN signal in a TD-CIMS caused by NO is tested and quantified.
- TD-CIMS is applicable for PAN measurement in urban areas with necessary correction.
- The PAN formation efficiency in urban Hong Kong increased with NO_2

concentration.

Graphic Abstract

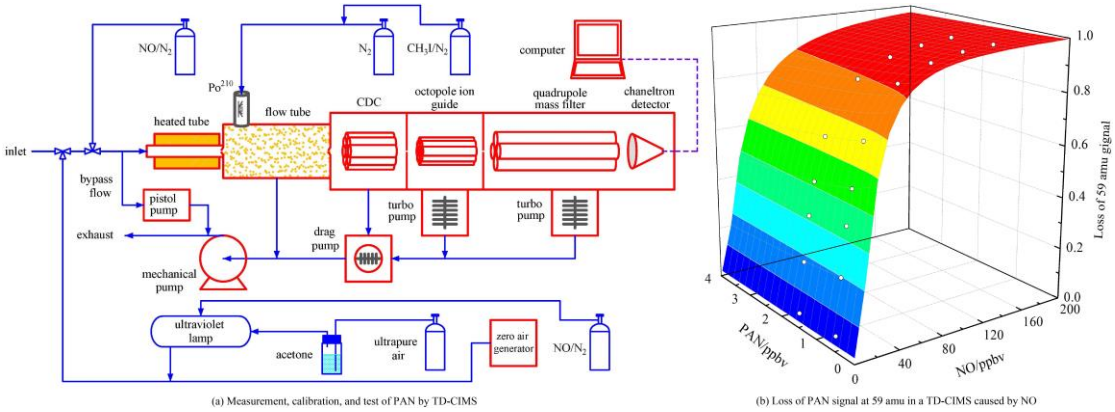

Abstract

Peroxyacetyl nitrate (PAN) is an important indicator of photochemical smog and has adverse effects on human health and vegetation growth. A rapid and highly selective technique of thermal dissociation–chemical ionization mass spectrometry (TD-CIMS) was recently developed to measure the abundance of PAN in real time; however, it may be subject to artifact in the presence of nitric oxide (NO). In this study, we tested the interference of the PAN signal induced by NO, evaluated the performance of TD-CIMS in an urban environment, and investigated the concentration and formation of PAN in urban Hong Kong. NO caused a significant underestimation of the PAN signal in TD-CIMS, with the underestimation increasing sharply with NO concentration and decreasing slightly with PAN abundance. A formula was derived to link the loss of PAN signal with the concentrations of NO and PAN, which can be used for data correction in PAN measurements. The corrected PAN data from

TD-CIMS were consistent with those from the commonly used gas chromatography with electron capture detection, which confirms the utility of TD-CIMS in an urban environment in which NO is abundant. In autumn of 2010, the hourly average PAN mixing ratio varied from 0.06 ppbv to 5.17 ppbv, indicating the occurrence of photochemical pollution in urban Hong Kong. The formation efficiency of PAN during pollution episodes was as high as 3.9 to 5.9 ppbv per 100 ppbv ozone. PAN levels showed a near-linear increase with NO_x concentration, suggesting a control policy of NO_x reduction for PAN pollution.

Keywords TD-CIMS, Peroxyacetyl nitrate, Interference, Photochemical pollution, Formation efficiency

1 Introduction

Peroxyacetyl nitrate (PAN), produced from photochemical reactions of volatile organic compounds in the presence of NO_x, is a major air pollutant in photochemical smog and acts as an indicator of photochemical pollution [1]. Being a strong oxidant, PAN affects human health, especially the eyes, skin, and respiratory system [2,3]. It also has adverse effects on vegetation by damaging leaves, thereby suppressing growth [4,5]. In addition, as one of the oxidation products of NO_x, PAN contributes a significant fraction of the total reactive odd nitrogen species in the boundary layer [6] and affects nitrogen recycling and long-range transport [7,8]. Because of its significant environmental effects, a number of studies have been conducted in

America, Europe, and Asia to investigate the concentrations and variations of PAN, to understand its origins and formation mechanisms, and finally to provide guidelines for PAN pollution control [9-11].

The measurement of PAN is commonly conducted with gas chromatography with electron capture detection (GC-ECD), which is a sensitive technique with relatively high temporal resolution (normally 5 to 10 minutes) that has been well developed and widely used in field studies on PAN in recent decades [12–14]. However, the ECD signals of PAN suffer from potential interference from other molecules with high electron affinity (e.g., halogenated hydrocarbons and organic nitrates) [14,15]. Furthermore, the great variability in PAN abundance, for example, in urban areas or during aircraft measurement, has highlighted the urgent need for a faster analytical technique [16]. With the wide use of mass spectrometry for on-line measurements of air pollutants [17], thermal dissociation–chemical ionization mass spectrometry (TD-CIMS) was recently developed by Slusher et al. to detect the concentrations of PAN and other peroxy acyl nitrates with high selectivity and a very high temporal resolution (as fast as several seconds) [18]. This technique has been successfully used in several field campaigns on pollution transport at Mount Bachelor Observatory [19], on eddy covariance flux above forests [20,21], and on PAN budget on a ponderosa pine plantation [22]. An optimized TD-CIMS has been well characterized by internal standard calibrations involving ^{13}C-labelled synthetic PAN and is capable of simultaneously measuring the abundances of PAN, peroxypropionyl nitrate (PPN), peroxyisobutyryl nitrate (PiBN), peroxy-n-butyryl nitrate (PnBN), peroxyacryloyl

nitrate (APAN), peroxycrotonyl nitrate (CPAN), and peroxymethacryloyl nitrate (MPAN) [15]. The fast mass spectrometry detection is particularly suitable for aircraft- and vehicle-carried measurements [23]. Despite these advantages, significant interference exists in PAN measurements due to the rapid reactions between the thermal dissociated radicals or reagent ions and the ambient trace gases. *Phillips et al.* (2013) has confirmed that peroxyacetic acid (PAA) interferes with PAN measurement by TD-CIMS with an error of ~4% [24]. Regarding the more abundant nitric oxide (NO) [15,18], determining the interference accurately requires careful testing and evaluation.

Urban areas are often characterized by intensive emissions of anthropogenic NO_x and volatile organic compounds due to the great amount of human activity and industrial production [25]. As a result, urban areas and their downwind regions are prone to suffer from photochemical pollution [26]. In this study, both laboratory tests and field measurements were conducted to quantify the underestimation in the PAN signal from TD-CIMS caused by NO interference and to evaluate the performance of TD-CIMS for PAN measurements in an urban environment with abundant NO. The concentrations and variations of PAN and related trace gases in urban Hong Kong in the autumn of 2010 are presented, and the formation efficiency of PAN during several pollution episodes is investigated in detail.

2 Experiment and methods

2.1 Laboratory and field measurements

The laboratory tests and field measurements were both conducted at an urban site in Hong Kong. Detailed information on the measurement site is given in our previous study [27]. Briefly, the site was situated at the Hong Kong Polytechnic University. To the south is a harbor and a cross-harbor tunnel. Therefore, when a south wind prevailed, a NO_x-rich plume appeared with a larger fraction of NO.

The laboratory tests were carried out by manually inputting certain concentrations of synthetic PAN with the addition of known concentrations of NO. The mixed gas samples were measured with TD-CIMS and other nitrogen oxide analyzers. The field measurements of PAN, related trace gases, and meteorological parameters began on Oct. 15, 2010 and ended on Dec. 5, 2010 during a period of severe photochemical pollution.

2.2 TD-CIMS configuration

The TD-CIMS deployed in this study was developed by the *L. Gregory Huey* group [18]. It is based on soft and selective ion-molecule reactions between the thermally dissociated products of the target compounds and the reagent ion, with the produced ions (or cluster ions) detected by mass spectrometry. Figure 1 presents a schematic diagram of the TD-CIMS used to measure the ambient PAN. Iodide ions were generated by passing a small flow of 0.3% CH_3I in nitrogen through an alpha source (Po-210, 370 MBq, *NRD*) and were used as the reagent ions. The counts of the reagent ion cluster $I(H_2O)^-$ were monitored throughout the campaign and were

normally in the range of 1.5–2.5×10^5 Hz. Air samples were drawn into the TD-CIMS at a flow rate of 1.5 standard liter per minute (SLPM) through a Teflon tube (3/8'' outside diameter), with an additional flow of 7.7 SLPM to the exhaust tube. The last part (15 cm in length) of the Teflon sampling inlet (before the flow tube) was heated to 180 ℃, leading to the complete thermo-decomposition of PAN (*R1*). The generated acetylperoxy radical ($CH_3C(O)O_2$) reacted with I^- in the flow tube at ~20 Torr. The produced acetate ions (via *R2*) passed through a collisional dissociation chamber with an axial electric field of ~25 V cm^{-1} at <0.5 Torr and were then detected with a quadruple mass spectrometer at 59 *amu*. Note that the same TD-CIMS was also used to measure the sum of dinitrogen pentoxide and nitrate radical (N_2O_5+NO_3) at 62 *amu* in this field campaign [27].

$$CH_3C(O)O_2NO_2 + M \rightarrow CH_3C(O)O_2 + NO_2 + M \qquad (R1)$$

$$CH_3C(O)O_2 + I^- \rightarrow CH_3C(O)O^- + IO \qquad (R2)$$

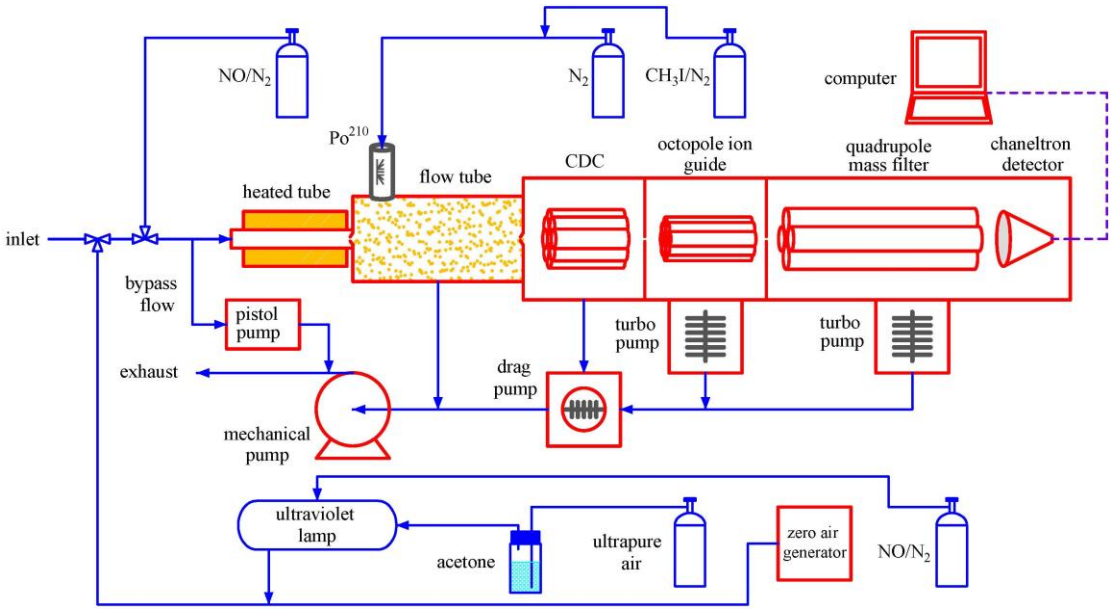

Fig. 1 Schematic diagram of the TD-CIMS used for laboratory tests and field measurements.

Figure 2 shows the signal peak of the mass-to-charge ratio at 59 *amu*, which was well separated from the adjacent peaks. Note that the ion-molecule reaction products of thermal dissociated peroxy radicals of APAN, PPN, MPAN/CPAN, and PiBN/PnBN can also be detected at 71, 73, 85, and 87 *amu*, respectively; however, they are not included in this study due to the lack of standard sources for calibration.

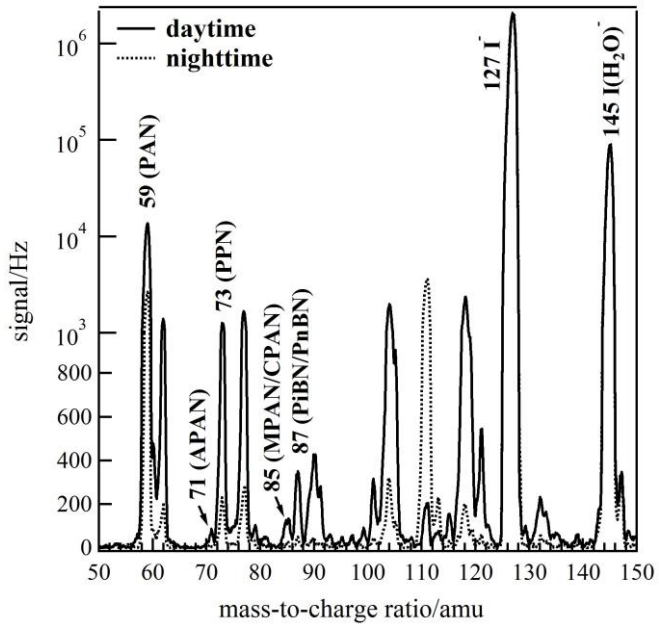

Fig. 2 Mass spectra of ambient air by TD-CIMS in urban Hong Kong during daytime and nighttime.

The background PAN signal at 59 *amu* was determined once per hour via addition of a small flow of NO (1000 ppm, 5 sccm) to the sample flow. The NO titrated acetylperoxy radicals and thus PAN. During the field measurement, the average background signal of PAN was 67.5 ± 38.4 Hz (mean ± SD), which was very low compared to the sample signal. The low background suggests that the measurement of PAN by TD-CIMS was little influenced by PAA in ambient air.

In this study, the sensitivity of PAN measured by TD-CIMS was calibrated once per

week by introducing diluted synthetic PAN in zero air. The PAN was synthesized from a PAN calibrator (*Meteorologie Consult GmbH*) based on the reactions between NO and the photolysis products of acetone in ultrapure air with a Pen-Ray lamp. The concentrations of PAN introduced to the TD-CIMS were determined simultaneously by a NO_x analyzer equipped with a blue-light converter and a NO_y analyzer equipped with a molybdenum converter (42CY, *Thermo Environmental Instruments (TEI*)). Figure 3 presents an example of PAN calibration conducted on the night of Nov. 14, 2010 with a reagent ion cluster $I(H_2O)^-$ of 1.5×10^5 Hz. Note that there was a significant positive offset in the scatterplot of the 59 *amu* signal versus the PAN concentration, which is mainly attributed to excess acetylperoxy radicals and the reaction products with RO_2 and HO_2 radicals in the calibration system. Therefore, when sampling the synthetic PAN from photolytic source, relative signals of 59 amu were used (*i.e.*, deducting the "background" at zero PAN concentration). During the field measurements in urban Hong Kong, the average (±SD) sensitivity of TD-CIMS for PAN was 3.5 ± 0.7 Hz/pptv. Based on this sensitivity and three times the SD of the background signal, the typical detection limit of PAN over a 6-second average time was estimated to be 33 pptv in an urban environment. It was noticed that the temperature in the flow tube could apparently influence the effective rates of the ion-molecule reactions and thus alter the sensitivity. To avoid significant variation in the PAN sensitivity, for this study, two air conditioners were installed at the measurement site to keep the room at a constant temperature, and the flow tube was packed with insulation materials to reduce heat loss. However, the variation in the

reagent ion cluster abundance during the measurement periods and the difference from that during calibrations are sources of some uncertainty in the measurement data [15].

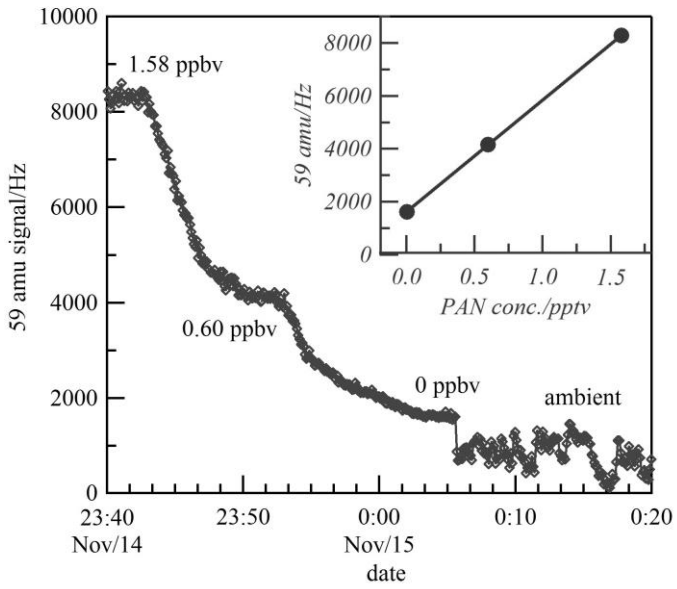

Fig. 3 Raw signal at 59 amu for PAN calibration in the night of Nov. 14, 2010. Insert shows the calibration curve.

2.3 Ancillary instruments

Several other instruments were also used in this study. To evaluate the performance of TD-CIMS in an urban environment, the ambient PAN concentration was simultaneously determined with a commercially available GC-ECD PAN-Analyzer (*Meteorologie Consult GmbH*). The detection limit of the GC-ECD analyzer was 50 pptv, with an uncertainty of 15%. A detailed introduction to GC-ECD PAN-Analyzer can be seen in our previous study [28]. Ozone was analyzed by the UV photometric method (49i, *TEI*). NO and NO_2 were measured using a chemiluminescence technique (42i, *TEI*) coupled with a blue light converter (*Air Quality Design*) [29]. Solar

198 radiation and the temperature were determined with a pyranometer (LI-200, *LI-COR*)
199 and a temperature probe (41382VC/VF, *M.R. YOUNG*), respectively.
200
201 # 3 Results and discussion
202
203 ## 3.1 Interference caused by NO and data correction
204 NO causes major interference in the measurement of ambient PAN in TD-CIMS. It
205 depletes the PAN signal at 59 *amu* (i.e., the signal of the acetate ion) due to the fast
206 reaction between acetylperoxy radicals and NO in the heated inlet and thus causes
207 underestimation of the measured PAN data [18]. To examine the degree of
208 interference of the PAN signal caused by NO, tests were conducted in the laboratory
209 by sampling a mixed gas of synthetic PAN in levels of 0.61 and 1.62 ppbv with
210 different concentrations of NO: 0, 5, 10, 20, 30, 60, 90, 120, and 150 ppbv.
211 The interference tests demonstrate the remarkable loss in the PAN signal by
212 TD-CIMS, which increased sharply with the NO concentration and decreased slightly
213 with the PAN abundance (as shown in Fig. 4). For 1.62 ppbv PAN, the loss of the
214 PAN signal increased to 23% when the NO concentration was 10 ppbv, and it reached
215 83% when the NO concentration was 50 ppbv. Note that the observed loss was higher
216 than that estimated by *Slusher et al.* [18]. Based on the test results, a formula (*Eq1*) is
217 derived here to describe the quantitative relationship of the loss percentage with the
218 concentrations of NO and PAN in the sample flow (both in ppbv).

219 $$\mathrm{Loss} = 1 - 0.98 \times e^{-\left(ln([NO]\div 3.85)+\left(1.65+0.0137\times(1000\times[PAN])^{0.418}\right)\right)^2} \quad \text{(Eq1)}$$

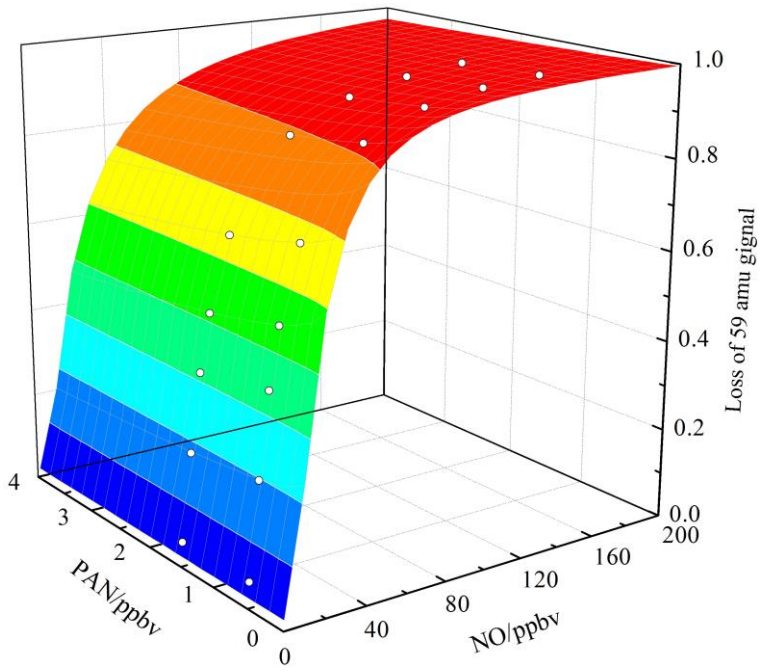

Fig. 4 The effect of NO and PAN concentration on signal loss at 59 amu.

During field measurements in urban Hong Kong, the NO concentration was very high during late autumn, with an average mixing ratio of 21.6 ppbv. Consistent with the laboratory tests, a remarkable loss (a sharp trough) in the PAN signal was frequently observed during high-NO conditions in the morning. To evaluate the performance of TD-CIMS in PAN measurements in an urban environment with consideration of NO interference, the original PAN data from TD-CIMS were corrected with *Eq1*. The corrected PAN data were calculated with an iterative method, that is, by repeatedly inputting the outputted PAN value until they were almost the same (less than 1% difference in PAN concentration between two consecutive calculations). After correction, the measured PAN concentrations from TD-CIMS agreed well with those determined from the GC-ECD PAN Analyzer (slope = 0.98 and R^2 = 0.91 for the hourly average data; see Fig. 5). This agreement confirms that the NO reaction was responsible for most of the interference in the PAN

measurements by TD-CIMS and that the derived formula can be used for data correction.

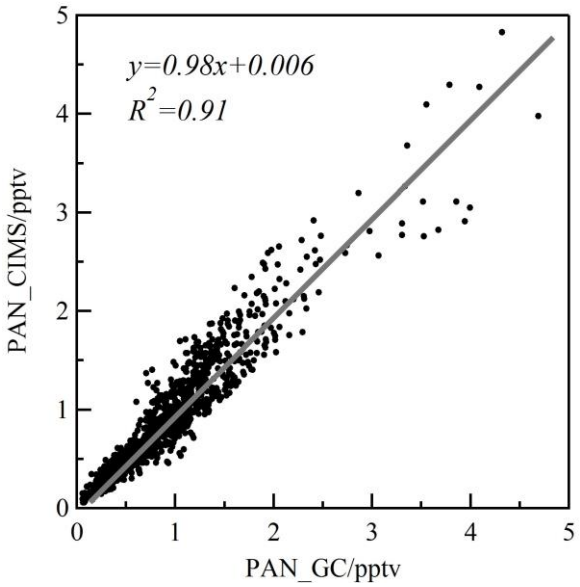

Fig. 5 Scatter plot of corrected PAN concentration by TD-CIMS versus that by GC-ECD.

Overall, TD-CIMS is a reliable technique to determine the atmospheric PAN in an urban environment with necessary correction. In addition, the field measurements of PPN, APAN, MPAN/CPAN, and PiBN/PnBN by TD-CIMS are also believed to be feasible in an urban atmosphere if standard sources are available.

3.2 Concentrations and variations

Figure 6 presents the time series of the PAN concentration measured by TD-CIMS (after correction for the interference caused by NO, as with the data below), the mixing ratios of related trace gases, and the meteorological parameters at the urban area in Hong Kong between Oct. 15 and Dec. 5, 2010. As shown, the PAN concentration in urban Hong Kong exhibited large variations, with a maximum hourly

concentration of 5.17 ppbv and a minimum close to the detection limit. During the 50-day measurement period (excluding 11 Nov. due to a lack of data), there were 3 days in which the peak PAN concentration exceeded 4 ppbv and 14 days in which the peak PAN concentration was above 2 ppbv. Generally, the PAN concentration peaks appeared with elevated levels of ozone, moderately high levels of NO_2, and low concentrations of NO, in combination with intensive solar radiation and high temperature (above 24 ℃). During the entire sampling period, the average concentration of PAN at this urban site was 0.90 ppbv, comparable to or slightly lower than those at urban sites in Beijing, Seoul, and Los Angeles [11,30,31] but substantially higher than that measured during the same season at a background site in southeast Hong Kong [32]. The relatively high levels of PAN observed in this study confirm the severe photochemical pollution during autumn in Hong Kong and suggest that there is a potential hazard to human health and vegetation production from PAN and other photochemical oxidants.

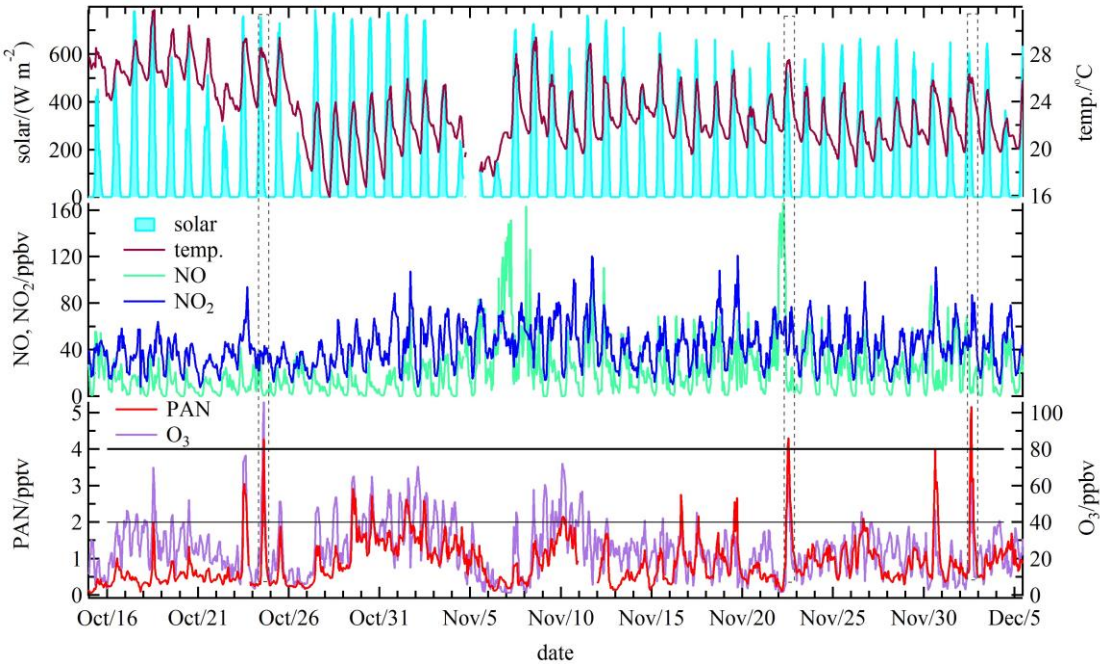

Fig. 6 Time series of concentrations of PAN, O_3, NO, and NO_2, and meteorological parameters of solar radiation and temperature for the field measurements.

The average diurnal profiles of PAN and other trace gases are shown in Fig. 7. As depicted, PAN presents a broad concentration peak in the early afternoon, with a maximum value of 1.46 ppbv at 14:00 local time. PAN reached a maximum at the same time as ozone, because both were produced from photochemical reactions involving volatile organic compounds and NO_x. NO_2 and NO presented two concentration peaks during the morning and late afternoon rush hours. When the NO concentration peaks appeared, there were two valleys in the O_3 concentration but not in the PAN concentration.

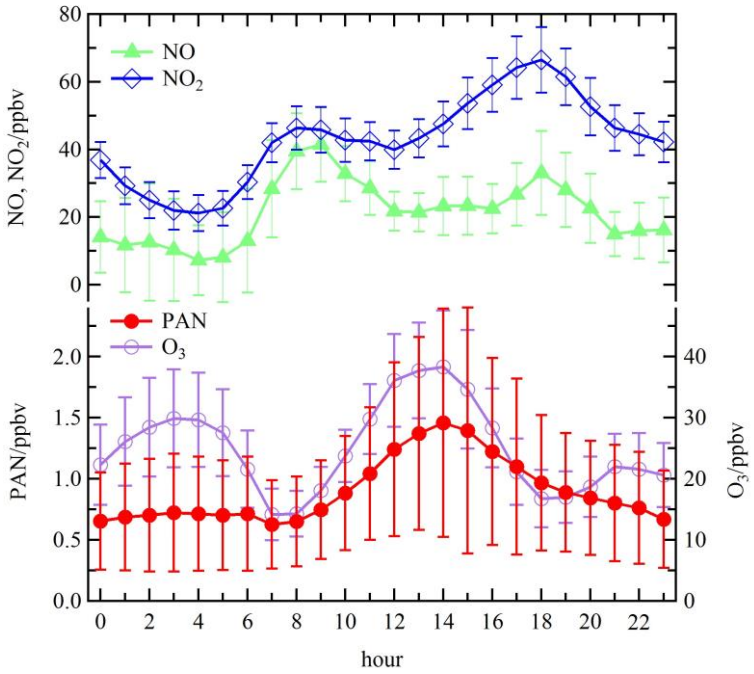

Fig. 7 Diurnal variation of PAN, O_3, NO, and NO_2 for the field measurements. Error bars represent half of the standard error.

3.3 Formation efficiency during pollution episodes

Both PAN and ozone are produced from photochemical processes involving NO_x and VOCs. However, they have different precursor VOCs and production efficiencies. The photochemical production efficiencies of PAN and ozone can be reflected in the correlation between them. To understand the formation efficiency of PAN in urban Hong Kong, scatterplots were drawn to show the relationship between PAN and ozone during the daytime period (10:00 to 19:59 local time) for the 3 most polluted episodes (Oct. 24, Nov. 22, and Dec. 2). As shown in Fig. 8, the PAN concentration exhibited a very high correlation with the ozone mixing ratio ($R^2 > 0.8$). The slope of PAN versus ozone was in the range of 0.039 to 0.059, indicating that 3.9 to 5.9 ppbv PAN was produced when 100 ppbv ozone formed via photochemical reactions. Furthermore, the PAN formation efficiency increased nearly linearly with the NO_2 level. During the daytime of Oct. 24, Nov. 22, and Dec. 2, the relative formation efficiency of PAN was 3.9, 5.1, and 5.9 ppbv per 100 ppbv ozone, respectively, with concurrent average NO_x concentrations of 44.4, 60.4, and 67.1 ppbv, respectively. The PAN formation efficiency in urban Hong Kong was comparable with those observed in urban and suburban areas in China (e.g., Beijing, Lanzhou) [11,28,33] but significantly higher than those observed at rural, coastal, and mountain sites [32,34,35]. The enhanced PAN formation and PAN concentration caused by elevated levels of NO_x in urban areas emphasize the need to reduce NO_x emissions to mitigate PAN pollution in Hong Kong.

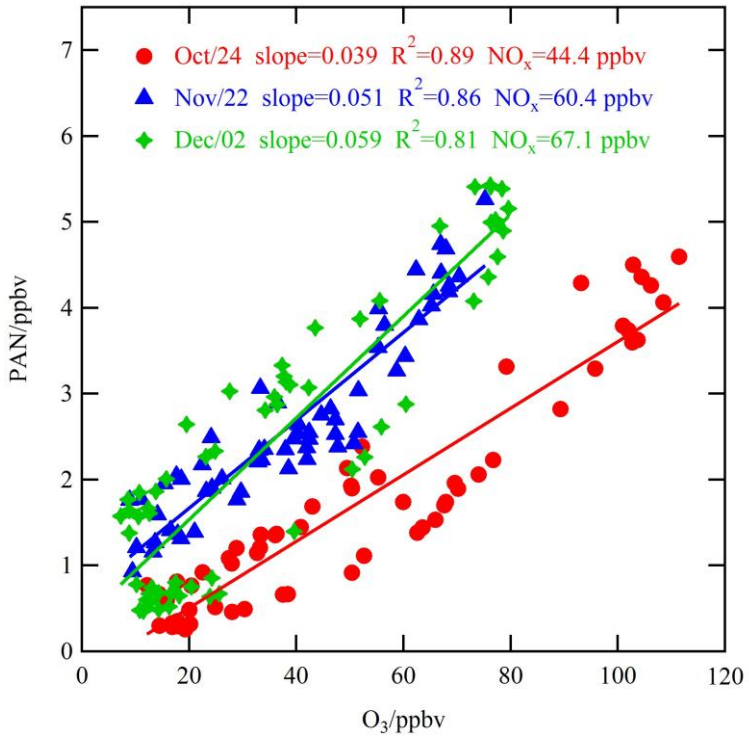

Fig. 8 Scatter plots of PAN versus ozone for three pollution episodes on Oct. 24, Nov. 22, and Dec. 2, 2010. The slope indicates the relative formation efficiency of PAN.

4 Summary and conclusions

Laboratory tests and field measurements of PAN were conducted to evaluate the interference and performance of the recently developed TD-CIMS in an urban environment and to understand the abundances and formation of PAN in urban Hong Kong. The underestimation of PAN signals at 59 *amu* by TD-CIMS was examined by adding known concentrations of NO to synthetic PAN. The loss of the PAN signal was rather large in the presence of NO. For 1.62 ppbv PAN, when NO was 10 and 50 ppbv, the loss reached 23% and 83%, respectively. According to the test results, a formula was derived to quantify the relationship between the PAN signal loss and the concentrations of NO and PAN, which can be used to correct the PAN data detected

315 by TD-CIMS. After correction, the PAN data obtained from TD-CIMS agreed well
316 with those measured by GC-ECD, indicating that TD-CIMS is generally a reliable
317 technique with very high temporal resolution for PAN measurements in an urban
318 atmosphere. During field measurements in autumn of 2010, the average concentration
319 of PAN in urban Hong Kong was 0.91 ppbv, with a maximum hourly value of 5.17
320 ppbv. The moderately high concentrations of PAN demonstrate the presence of
321 photochemical pollution in the study area. The concentration peak of PAN usually
322 appeared in the early afternoon, corresponding to the ozone peaks. In the three severe
323 pollution episodes with peak PAN above 4 ppbv, the relative formation efficiency of
324 PAN was in the range of 3.9 – 5.9 ppbv per 100 ppbv ozone. The PAN formation
325 efficiency rose almost linearly with NO_x abundance, highlighting the need to control
326 NO_x to mitigate PAN pollution in Hong Kong.
327

328 ## 5 Acknowledgments

329 This work was supported by the Environment and Conservation Fund of Hong Kong
330 (Project No. 2009-07), National Natural Science Foundation of China (Nos. 41275123,
331 21407094, 91544213), China Postdoctoral Science Foundation (No. 2014M561932),
332 and the Jiangsu Collaborative Innovation Center for Climate Change. The authors
333 thank Dr. Pamela Holt for proofreading the manuscript.
334

335 ## 6 References

336 1. Stephens E R. The formation, reactions, and properties of peroxyacyl nitrates

(PANs) in photochemical air pollution. Advances in Environmental Science and Technology, 1969, 1: 119-146.

2. Vyskocil A, Viau C, Lamy S. Peroxyacetyl nitrate: review of toxicity. Human & Experimental Toxicology, 1998, 17(4): 212-220

3. Parrish D D, Xu J, Croes B, Shao M. Air quality improvement in Los Angeles—perspectives for developing cities. Frontiers of Environmental Science & Engineering, 2016, 10(5): 11, doi: 10.1007/s11783-016-0859-5

4. Taylor O C. Importance of Peroxyacetyl Nitrate (PAN) as a Phytotoxic Air Pollutant. Journal of the Air Pollution Control Association, 1969, 19(5): 347-351

5. Temple P J, Taylor O C. World-wide ambient measurements of peroxyacetyl nitrate (PAN) and implications for plant injury. Atmospheric Environment (1967), 1983, 17(8): 1583-1587

6. Ridley B A, Shetter J D, Gandrud B W, Salas L J, Singh H B, Carroll M A, Hübler G, Albritton D L, Hastie D R, Schiff H I, Mackay G I, Karechi D R, Davis D D, Bradshaw J D, Rodgers M O, Sandholm S T, Torres A L, Condon E P, Gregory G L, Beck S M. Ratios of Peroxyacetyl Nitrate to Active Nitrogen Observed During Aircraft Flights Over the Eastern Pacific Oceans and Continental United States. Journal of Geophysical Research, 1990, 95(D7): 10179-10192

7. Singh H B, Salas L J, Ridley B A, Shetter J D, Donahue N M, Fehsenfeld F C, Fahey D W, Parrish D D, Williams E J, Liu S C, Hubler G, Murphy P C. Relationship between peroxyacetyl nitrate and nitrogen oxides in the clean

troposphere. Nature, 1985, 318(6044): 347-349

8. Orlando J J, Tyndall G S, Calvert J G. Thermal decomposition pathways for peroxyacetyl nitrate (PAN): Implications for atmospheric methyl nitrate levels. Atmospheric Environment. Part A. General Topics, 1992, 26(17): 3111-3118
9. Singh H B, Salas L J, Viezee W. Global distribution of peroxyacetyl nitrate. Nature, 1986, 321(6070): 588-591
10. Gaffney J S, Marley N A, Cunningham M M, Doskey P V. Measurements of peroxyacyl nitrates (PANS) in Mexico City: implications for megacity air quality impacts on regional scales. Atmospheric Environment, 1999, 33(30): 5003-5012
11. Zhang J B, Xu Z, Yang G, Wang B. Peroxyacetyl nitrate (PAN) and peroxypropionyl nitrate (PPN) in urban and suburban atmospheres of Beijing, China. Atmospheric Chemistry and Physics Discussions, 2011, 11(3): 8173-8206
12. Williams J, Roberts J M, Bertman S B, Stroud C A, Fehsenfeld F C, Baumann K, Buhr M P, Knapp K, Murphy P C, Nowick M, Williams E J. A method for the airborne measurement of PAN, PPN, and MPAN. Journal of Geophysical Research, 2000, 105(D23): 28943-28960
13. Flocke F, Weinheimer A, Swanson A, Roberts J, Schmitt R, Shertz S. On the measurement of PANs by gas chromatography and electron capture detection. Journal of Atmospheric Chemistry, 2005, 52(1): 19-43
14. Zhang G, Mu Y, Liu J, Mellouki A. Direct and simultaneous determination of trace-level carbon tetrachloride, peroxyacetyl nitrate, and peroxypropionyl nitrate using gas chromatography-electron capture detection. Journal of Chromatography

A, 2012, 1266: 110-115

15. Zheng W, Flocke F M, Tyndall G S, Swanson A, Orlando J J, Roberts J M, Huey L G, Tanner D J. Characterization of a thermal decomposition chemical ionization mass spectrometer for the measurement of peroxy acyl nitrates (PANs) in the atmosphere. Atmospheric Chemistry and Physics, 2011, 11(13): 6529-6547
16. Hastie D R, Gray J, Langford V S, Maclagan R G A R, Milligan D B, McEwan M J. Real-time measurement of peroxyacetyl nitrate using selected ion flow tube mass spectrometry. Rapid Communications in Mass Spectrometry, 2010, 24(3): 343-348
17. Huey L. Measurement of trace atmospheric species by chemical ionization mass spectrometry: Speciation of reactive nitrogen and future directions. Mass Spectrometry Reviews, 2007, 26(2): 166-184
18. Slusher D L, Huey L G, Tanner D J, Flocke F M, Roberts J M. A thermal dissociation-chemical ionization mass spectrometry (TD-CIMS) technique for the simultaneous measurement of peroxyacyl nitrates and dinitrogen pentoxide. Journal of Geophysical Research, 2004, 109(D19): D19315, doi: 10.1029/2001gl013443
19. Wolfe G M, Thornton J A, McNeill V F, Jaffe D A, Reidmiller D, Chand D, Smith J, Swartzendruber P, Flocke F, Zheng W. Influence of trans-Pacific pollution transport on acyl peroxy nitrate abundances and speciation at Mount Bachelor Observatory during INTEX-B. Atmospheric Chemistry and Physics, 2007, 7(20): 5309-5325

403 20. Turnipseed A A, Huey L G, Nemitz E, Stickel R, Higgs J, Tanner D J, Slusher D L,
404 Sparks J P, Flocke F, Guenther A. Eddy covariance fluxes of peroxyacetyl nitrates
405 (PANs) and NOy to a coniferous forest. Journal of Geophysical Research:
406 Atmospheres, 2006, 111(D9): D09304, doi: 10.1029/2005jd006631
407 21. Wolfe G M, Thornton J A, Yatavelli R L N, McKay M, Goldstein A H, LaFranchi
408 B, Min K E, Cohen R C. Eddy covariance fluxes of acyl peroxy nitrates (PAN,
409 PPN and MPAN) above a Ponderosa pine forest. Atmospheric Chemistry and
410 Physics, 2009, 9(2): 615-634
411 22. LaFranchi B, Wolfe G, Thornton J, Harrold S, Browne E, Min K, Wooldridge P,
412 Gilman J, Kuster W, Goldan P. Closing the peroxy acetyl nitrate budget:
413 observations of acyl peroxy nitrates (PAN, PPN, and MPAN) during BEARPEX
414 2007. Atmospheric Chemistry and Physics, 2009, 9(19): 7623-7641
415 23. Roiger A, Aufmhoff H, Stock P, Arnold F, Schlager H. An aircraft-borne chemical
416 ionization - ion trap mass spectrometer (CI-ITMS) for fast PAN and PPN
417 measurements. Atmospheric Measurement Techniques, 2011, 4(2): 173-188
418 24. Phillips G J, Pouvesle N, Thieser J, Schuster G, Axinte R, Fischer H, Williams J,
419 Lelieveld J, Crowley J N. Peroxyacetyl nitrate (PAN) and peroxyacetic acid (PAA)
420 measurements by iodide chemical ionisation mass spectrometry: first analysis of
421 results in the boreal forest and implications for the measurement of PAN fluxes.
422 Atmos. Chem. Phys, 2013, 13(3): 1129-1139
423 25. Wang Z, Shao M, Chen L, Tao M, Zhong L, Chen D, Fan M, Wang Y, Wang X.
424 Space view of the decadal variation for typical air pollutants in the Pearl River

425 Delta (PRD) region in China. Frontiers of Environmental Science & Engineering,
426 2016, 10(5): 9, doi: 10.1007/s11783-016-0853-y
427 26. Xue L, Wang T, Wang X, Blake D R, Gao J, Nie W, Gao R, Gao X, Xu Z, Ding A,
428 Huang Y, Lee S, Chen Y, Wang S, Chai F, Zhang Q, Wang W. On the use of an
429 explicit chemical mechanism to dissect peroxy acetyl nitrate formation.
430 Environmental Pollution, 2014, 195(2014): 39-47
431 27. Wang X, Wang T, Yan C, Tham Y J, Xue L, Xu Z, Zha Q. Large daytime signals
432 of N_2O_5 and NO_3 inferred at 62 amu in a TD-CIMS: chemical interference or a
433 real atmospheric phenomenon? Atmospheric Measurement Techniques, 2014,
434 7(1): 1-12
435 28. Zhang J, Wang T, Ding A, Zhou X, Xue L, Poon C, Wu W, Gao J, Zuo H, Chen J.
436 Continuous measurement of peroxyacetyl nitrate (PAN) in suburban and remote
437 areas of western China. Atmospheric Environment, 2009, 43(2): 228-237
438 29. Xu Z, Wang T, Xue L, Louie P K K, Luk C W Y, Gao J, Wang S, Chai F, Wang W.
439 Evaluating the uncertainties of thermal catalytic conversion in measuring
440 atmospheric nitrogen dioxide at four differently polluted sites in China.
441 Atmospheric Environment, 2013, 76(2013): 221-226
442 30. Lee G, Jang Y, Lee H, Han J-S, Kim K-R, Lee M. Characteristic behavior of
443 peroxyacetyl nitrate (PAN) in Seoul megacity, Korea. Chemosphere, 2008, 73(4):
444 619-628
445 31. Grosjean E, Grosjean D, Fraser M P, Cass G R. Air Quality Model Evaluation
446 Data for Organics. 3. Peroxyacetyl Nitrate and Peroxypropionyl Nitrate in Los

447 Angeles Air. Environmental Science & Technology, 1996, 30(9): 2704-2714
448 32. Xu Z, Xue L, Wang T, Xia T, Gao Y, Louie P K K, Luk C W Y. Measurements of
449 Peroxyacetyl Nitrate at a Background Site in the Pearl River Delta Region:
450 Production Efficiency and Regional Transport. Aerosol and Air Quality Research,
451 2015, 15(1): 833–841
452 33. Liu Z, Wang Y, Gu D, Zhao C, Huey L G, Stickel R, Liao J, Shao M, Zhu T, Zeng
453 L, Liu S C, Chang C C, Amoroso A, Costabile F. Evidence of Reactive Aromatics
454 As a Major Source of Peroxy Acetyl Nitrate over China. Environmental Science
455 & Technology, 2010, 44(18): 7017-7022
456 34. Zhang J M. Measurement of atmospheric peroxyacetyl nitrate (PAN) and the
457 implications to photochemical pollution. Hong Kong: The Hong Kong
458 Polytechnic University, 2009
459 35. Wang B, Shao M, Roberts J, Yang G, Yang F, Hu M, Zeng L, Zhang Y, Zhang J.
460 Ground-based on-line measurements of peroxyacetyl nitrate (PAN) and
461 peroxypropionyl nitrate (PPN) in the Pearl River Delta, China. International
462 Journal of Environmental and Analytical Chemistry, 2010, 90(7): 548-559